Hindawi Publishing Corporation
Journal of Sensors
Volume 2016, Article ID 6584650, 7 pages
http://dx.doi.org/10.1155/2016/6584650

Hindawi

Research Article

Modeling, Design, and Fabrication of Self-Doping $Si_{1-x}Ge_x$/Si Multiquantum Well Material for Infrared Sensing

Bo Jiang,[1] Dandan Gu,[2] Yulong Zhang,[2] Yan Su,[1] Yong He,[1] and Tao Dong[3]

[1] *Mechanical Engineering School, Nanjing University of Science and Technology, Nanjing, China*
[2] *Pen-Tung Sah Institute of Micro-Nano Science and Technology, Xiamen University, Xiamen, China*
[3] *Department of Micro and Nano Systems Technology (IMST), Faculty of Technology and Maritime Sciences, Buskerud and Vestfold University College, Raveien 205, 3184 Borre, Norway*

Correspondence should be addressed to Dandan Gu; gdd@xmu.edu.cn, Yulong Zhang; zyl98@xmu.edu.cn, and Tao Dong; tao.dong@hbv.no

Received 17 September 2015; Accepted 22 October 2015

Academic Editor: Wei Cao

Copyright © 2016 Bo Jiang et al. This is an open access article distributed under the Creative Commons Attribution License, which permits unrestricted use, distribution, and reproduction in any medium, provided the original work is properly cited.

The paper presents the study of band distributions and thermoelectric properties of self-doping $Si_{1-x}Ge_x$/Si multiquantum well material for infrared detection. The simulations of different structures (including boron doping, germanium concentrations, and SiGe layer thickness) have been conducted. The critical thickness of SiGe layer grown on silicon substrate has also been illustrated in the paper. The self-doping $Si_{1-x}Ge_x$/Si multiquantum well material was epitaxially grown on SOI substrate with reduced pressure chemical vapor deposition. Each layer of the material is clear in the SEM. The I-V characterizations and temperature resistance coefficient (TCR) tests were also performed to show the thermoelectric properties. The TCR was about −3.7%/K at room temperature in the experiments, which is competitive with the other thermistor materials. The material is a low noise material, whose root mean square noise is 1.89 mV in the experiments.

1. Introduction

Bolometer, one of uncooled infrared detectors, has been widely developed since 1992, when the "bridge structure" was reported by Honeywell. Bolometers are thermal infrared sensors that absorb electromagnetic radiation (8–14 μm) and thus increase their temperature [1–4]. The materials with high TCR (temperature resistance coefficient) are preferred to increase the sensitivity. Vanadium oxide and amorphous silicon are the most successful materials and occupy the major commercial market share [5]. The bolometer pixel size is developed to 17 μm, while the resolution is to 1920 × 1080 or even more [6, 7]. As a result of technical development, the next generation of bolometer should be combined with standard CMOS based integrated circuits to decrease the cost. However, vanadium is one of deep level pollution elements for the IC process [8, 9]. The special process line should be provided for vanadium oxide manufacture, which would be expensive in bolometer development. As a result, more and more researches have focused on the novel material with high TCR, which can also be compatible with IC industry. Various semiconductor materials are the most suitable materials among them. $Si_{1-x}Ge_x$/Si multiquantum wells (MQWs) have been proposed recently as a new thermistor material [10, 11]. Though the material has shown achieved good performance, it leads to some difficulties because of the practical growth process. With the rising complexity in this process, the cost and difficulties also increase to maintain the lattice quality.

In our previous works, the high TCR material with self-doping $Si_{1-x}Ge_x$/Si MQWs films was presented to solve the problems. The material has a thin buffer layer, where a proportion of boron atom diffusion is allowed [12]. This structure simplifies the process and can also promise a high lattice quality through epitaxial growth processes, such as the reduced pressure chemical vapor deposition (RPCVD) and molecular beam epitaxy (MBE). The works subsequently focus on the relationships between the energy bands modeling and doping distributions. The epitaxial processes were optimized and more characterizations about material noise were taken.

In the paper, the modeling of quantum well structures is introduced firstly. The band distributions of MQWs with different structures are calculated and illustrated in the part. The section also presents the epitaxial processes and characterization experiments. The SEM and electrical tests were conducted and shown in Section 3. The results show that the lattice of self-doping $Si_{1-x}Ge_x/Si$ multiquantum well material has good quality and the TCR is −3.7%/K, which is high compared with other material in the reports [13].

2. Energy Bands Modeling and Design

The resistance is temperature dependent for semiconductor. There is a close relationship between energy bands distributions and thermoelectric properties. The study of energy bans modeling is helpful to determine the MQWs structure. For p-type semiconductor, the carriers concentration follows [14]

$$p_0 = N_v e^{-(E_f - E_v)/kT}, \quad (1)$$

where E_f is Fermi level, E_v is valence band, k is Boltzmann's constant, T is temperature, and effective carriers concentration, N_v, is followed by

$$N_v = 2\left(\frac{2\pi m_p \times kT}{h^2}\right)^{3/2}, \quad (2)$$

where m_p is effective mass and h is Planck's constant.

Equation (1) illustrates the relationship between p-type semiconductor resistance and the temperature. The material TCR is defined as

$$\alpha = \frac{\partial R/\partial T}{R}, \quad (3)$$

where R is the resistance of the material, which is inversely proportional to the hole concentration, p_0, for the p-doped semiconductor. Equation (4) can be derived by (1) to (3) as

$$\alpha = -\frac{1}{kT^2}\left(\frac{3}{2}kT + E_f - E_v\right). \quad (4)$$

Equation (4) indicates the critical principle between the energy bands and the electrical properties of p-type semiconductors. As shown in (4), TCR increases with the rise of the distance from the Fermi level to the valence band.

The structures of Si/SiGe multiquantum wells and the corresponding valence energy bands are illustrated in Figure 1. The valence bands are split to heavy hole (HH), light hole (LH), and spin-split-off (SO) bands, where each band has two states, that is, spin-up and spin-down [15]. For cooled infrared detector, the photons transit from HH to LH or other energy levels, where the energy differences are consistent with the wavelength of infrared incidence. The process is a kind of photon-electrical effects, which needs pretty low working temperatures (e.g., 77 K) to depress the thermal noises [16]. For uncooled infrared detector, there is no effective photon-electrical process for the corresponding infrared incidence. The studies focus on increasing the energy gap between Fermi level and the valence band.

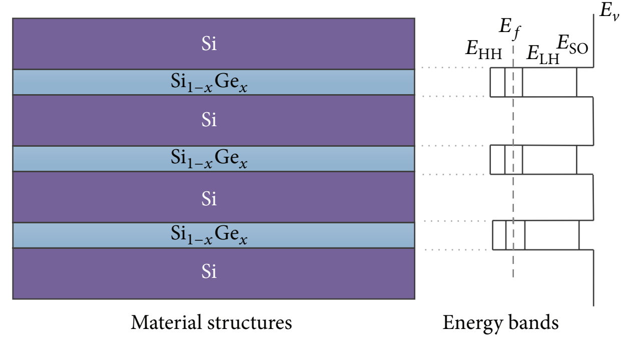

Figure 1: The structures of Si/SiGe multiquantum wells and the corresponding valence energy bands.

The valence barrier (silicon layer) is about 30 nm. It is big enough and there are few influences for quantum wells adjacently. Three points should be taken into account in Si/SiGe multiquantum wells design, which are listed as below:

(1) Boron doping distributions in quantum well structures.

(2) Quantum well, SiGe layer thickness of the material.

(3) Germanium concentration in SiGe layer.

The simulations results of valence energy bands with different boron doping distributions are carried out with the software NextNano^3, and the results were shown as Figure 2. In the simulation, the thickness and doping concentration (for both boron and germanium) of barriers and quantum well were defined. The simulation was conducted with no bias voltage. For self-doping structures, the boron doping distributions are similar in both Si layers and SiGe layers. The bands are curved due to high boron doping. The structures with lower doping (10^{18} cm^{-3}) obtain bigger differences between Fermi level and the valence band. The energy gap in Figure 2(a) is about 0.18 eV and the value is about 0.25 eV in Figure 2(b). The high boron doping only in SiGe layer achieves better performance. The energy gap is 3.6 eV in Figure 2(c) with 10^{19} cm^{-3} boron doping only in Si layer. However, it is impossible to achieve because the diffusion will happen in epitaxial process (process temperature is more than 600°C). The energy gap decreases when the boron doping decreases in SiGe layer as shown in Figure 2(d).

The thickness and the Ge concentration in SiGe layer are another two critical parameters to enhance TCR. The TCR increases with the increasing of Ge concentration and SiGe layer thickness as shown in Figure 3(a). High germanium achieves high TCR effectively. However, the lattice mismatch between silicon and germanium leads to strain or even dislocation or defects during epitaxial process. The epitaxial SiGe layer should be thinner than the critical thickness with corresponding Ge concentration on silicon substrate. The relationship between germanium concentration and the critical thickness is illustrated in Figure 3(b).

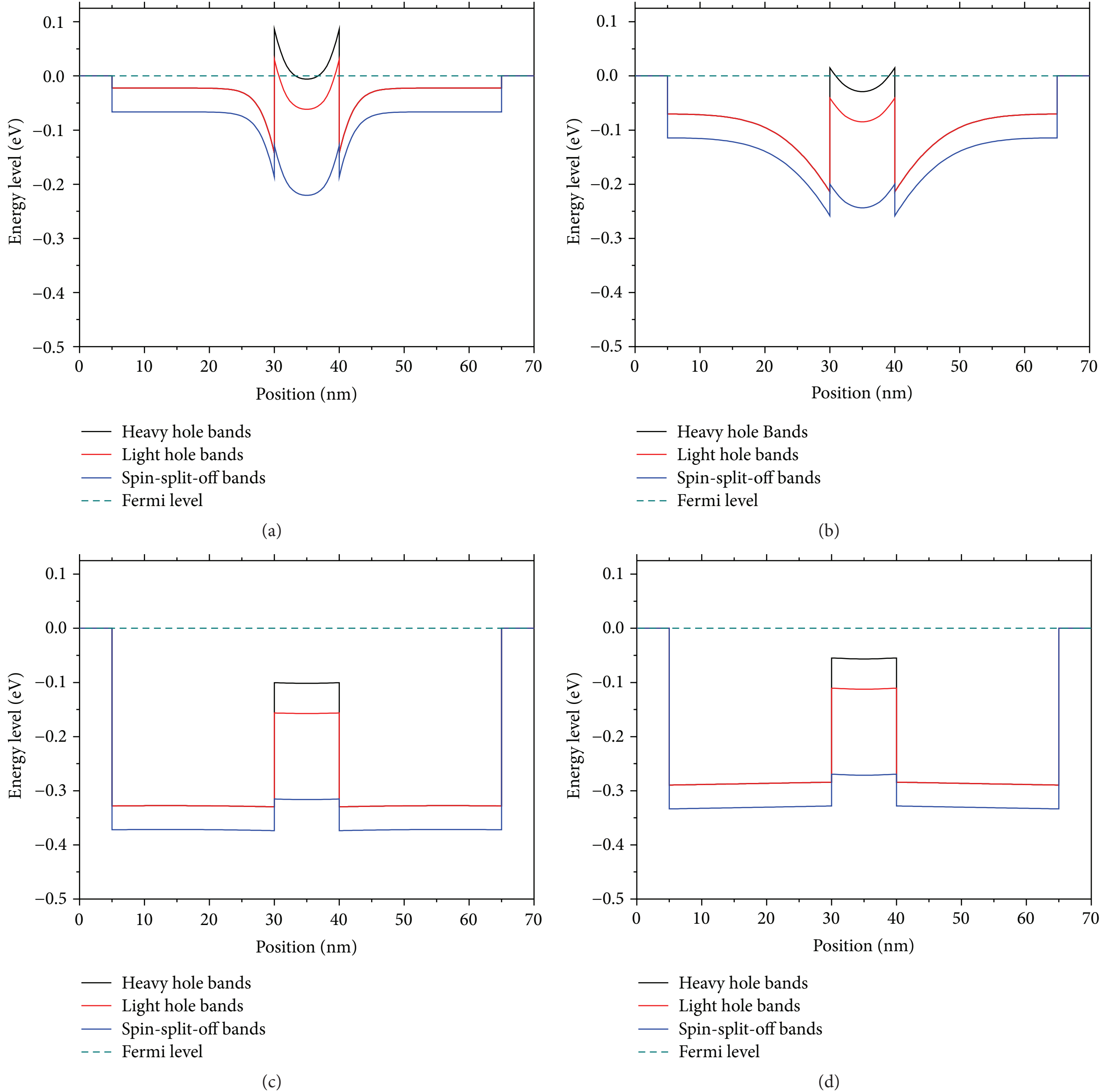

FIGURE 2: Valence energy bands of Si/SiGe quantum well with different boron doping: (a) 10^{19} cm^{-3} boron doping both in Si and in SiGe layers; (b) 10^{18} cm^{-3} boron doping both in Si and in SiGe layers; (c) 10^{19} cm^{-3} boron doping only in SiGe layer; (d) 10^{18} cm^{-3} boron doping only in SiGe layer.

3. Fabrication and Test

According to the design consideration described in Section 2, the SiGe layer with 10 nm and 30% germanium concentration is a compromising design for both performance and lattice quality. The Si/SiGe cycles with low boron doping achieve better energy bands bending and higher TCR. The self-doping $Si_{1-x}Ge_x$/Si multiquantum well material was grown on SOI substrate with reduced pressure chemical vapor deposition (RPCVD). In pretreatment, the samples were cleaned by *CRA-clean* method. Before the epitaxial growth processes, the temperature of the pretreatment chamber was raised to 950°C after filling it with a protective gas (H_2) until the pressure reached 10^{-2} Pa to remove the natural oxide layer on the top of the substrate wafers. In the epitaxial process, the disilane, germane, and borane were employed as sources and H_2 acted as diluent gas. The parameters in the process are listed in Table 1.

After epitaxial processes, characterizations have been conducted to test thermoelectric properties of the materials.

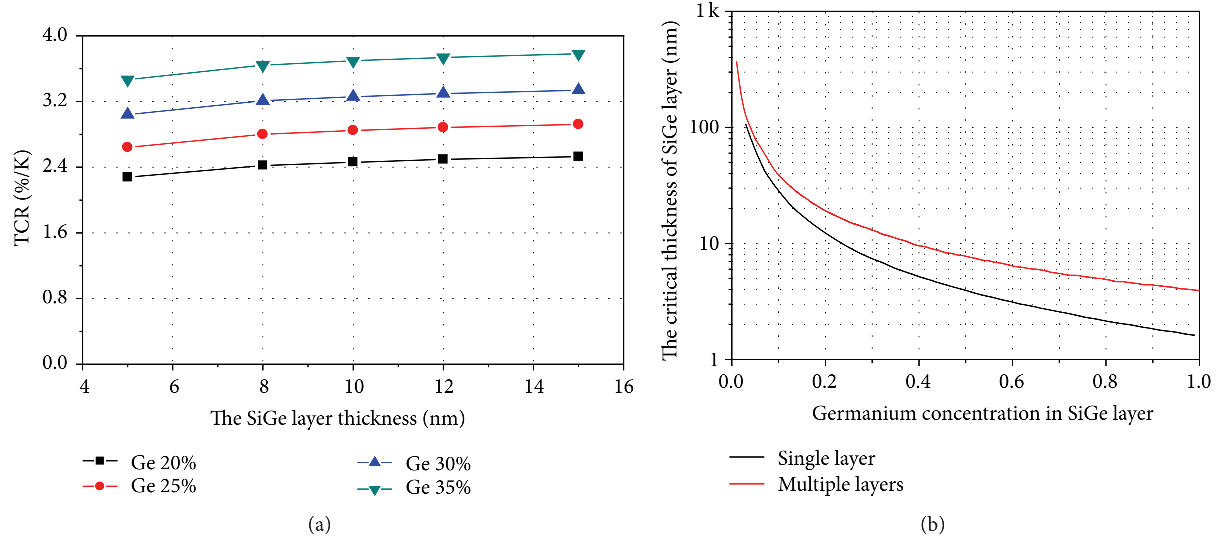

Figure 3: (a) The TCR of the structures with different germanium concentration and well thickness [11]; (b) the critical thicknesses with germanium concentration of SiGe layer growth on silicon substrate.

Table 1: Epitaxial process parameters of Si/SiGe MQWs with RPCVD.

Steps	Temperature (°C)	Sources	Flow (sccm)	Time	Comments
1	600	$Si_2H_6/BH_3/H_2$	6/1/80	30 min	High boron doping Si, 200 nm
2	600	Si_2H_6/H_2	6/60	9 min	Buffer layer, 60 nm
3	600	$Si_2H_6/GeH_4/H_2$	6/2.6/80	100 s	Si/SiGe cycles (30 nm/10 nm)
4	600	Si_2H_6/H_2	6/60	4.5 min	
5	600	$Si_2H_6/BH_3/H_2$	6/1/80	30 min	High boron doping Si, 200 nm

The test structures were processed and bonded as shown in Figures 4(a) and 4(c). The material was etched with SF_6 till high boron doping Si layer for electrical connection between two pads. The high boron doping silicon layer acted as electrical connection layer in the test and the current path is shown as illustrated in Figure 4(b). After that, Au wires were bonded on electrode pads to the packaging shell. *I-V* tests were conducted, and the results are shown as Figure 6.

4. Results and Discussion

The SEM of self-doping $Si_{1-x}Ge_x/Si$ multiquantum well material was shown as Figure 5. The material was grown on SOI substrate. In the figure, SiGe layers, which are only 10 nm thick for each layer, are shown clearly. The silicon layers without boron doping are 30 nm, which function as barrier layers in the quantum well structures. Buffer layer is about 35 nm and the boron atoms diffused into the multiquantum well structures in high temperature epitaxial process. High boron doping layers are about 150 nm as shown in the figure.

The noise tests were conducted and the lower frequency noise is dominant, such as $1/f$ noise and DC noise [17, 18]. The noise voltage is about $8\,mV/\sqrt{Hz}$ in low frequency and less than $0.01\,mV/\sqrt{Hz}$ in high frequency. The root mean square noise is 1.89 mV as calculations as shown in Figure 6.

Electrical characterizations have been conducted for thermoelectric properties of the materials after packaging. The *I-V* tests have been performed with different sized samples. The voltage was changing from −2 V to 2 V and the step is 0.04 V for each point. The experiments were performed at the room temperature. The results have been illustrated in Figure 7(a). The resistance decreases when the bias voltage rises. It is because the transient joule heat increases with higher bias voltage. The resistance increases with the decreasing of the sample size, which also follows the resistance law for multiquantum well structures.

The relationship between temperature and resistance of the samples is shown in Figure 7(b). The experiments were conducted at room temperature, which is also the working temperature for uncooled infrared detector. The sample with smaller size has better thermal-sensitive characteristics compared with the larger one as the results. The TCR of the samples are −3.7%/K and −3.1%/K, respectively, as the calculations with (3). It is high compared with other material in the reports [12].

5. Conclusions

The paper presents the modeling and design of self-doping $Si_{1-x}Ge_x/Si$ multiquantum well material. The design with

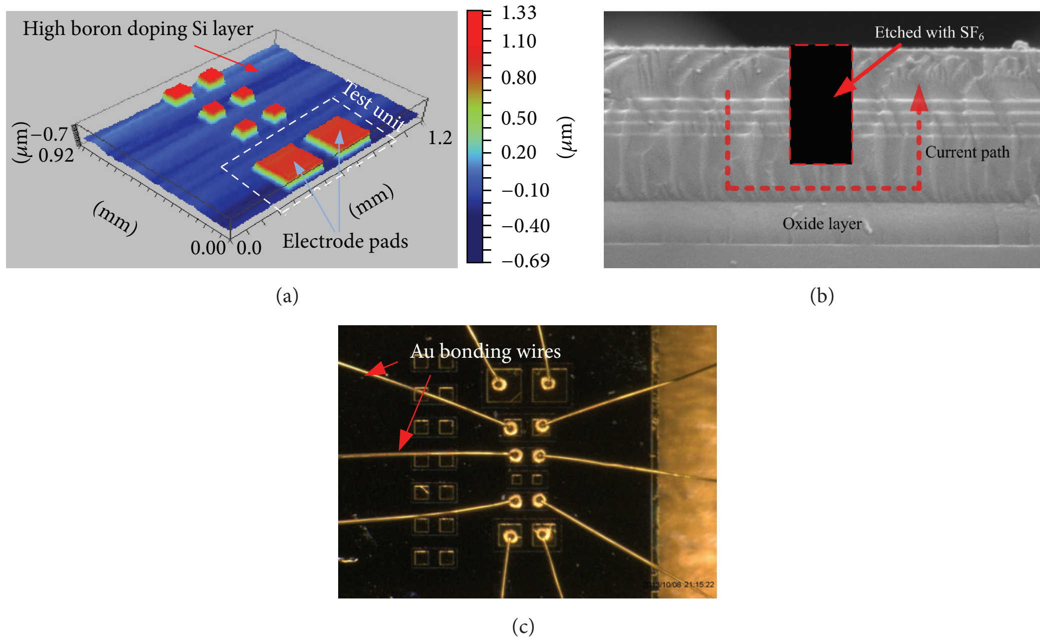

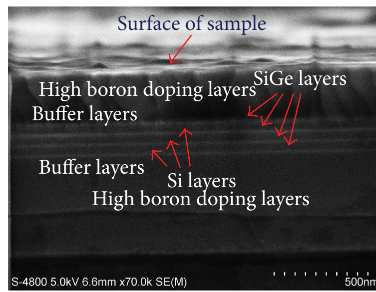

FIGURE 4: (a) The 3D profiler image of test structures after processes; (b) the current path in the I-V test experiments; (c) bonding with Au wire in the packaging.

FIGURE 5: The SEM of self-doping $Si_{1-x}Ge_x/Si$ multiquantum well material.

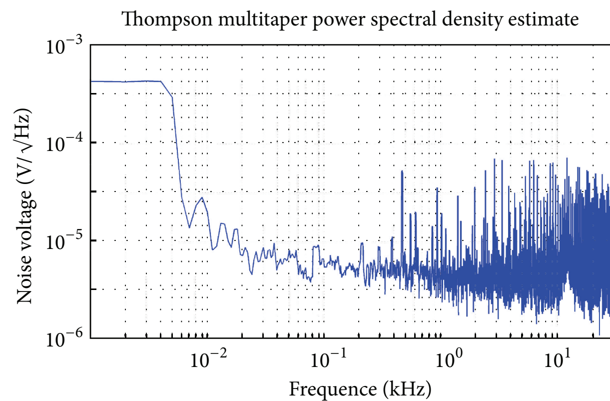

FIGURE 6: Noise power spectral density for the material.

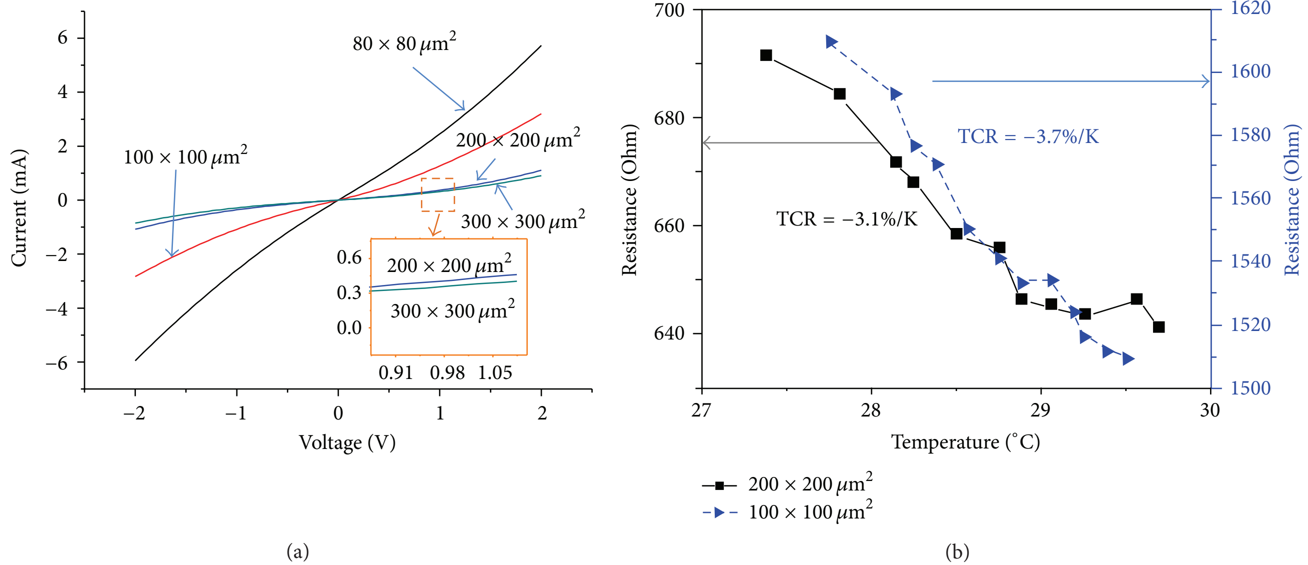

Figure 7: (a) *I-V* relationships with different sizes samples; (b) resistances with different temperature from 27°C to 30°C in TCR tests.

self-doping structure simplifies the process and can also promise a high lattice quality in epitaxial processes. Compared with our works previously, the band distributions and bends were discussed in the paper. The relationship between energy bands modeling and boron doping distributions, quantum well thickness, and Ge concentrations was illustrated in Section 2. The experiments of material epitaxial processes and thermoelectric characterizations were performed. The SEM in the paper shows the good quality of the material growth by RPCVD. The material has good thermal-electrical and low noise performances, which were proved by experiments. The TCR of the samples are −3.7%/K and −3.1%/K, respectively, in the experiments. The noise power spectral density experiment was conducted, and the RMS is 1.89 mV as calculations. The material with high TCR and low noise is also promising to apply in the other exothermic reactions detection.

Conflict of Interests

The authors declare no conflict of interests.

Acknowledgments

This work is supported by the Scientific Research Project (no. A2620110012).

References

[1] F. Niklaus, C. Vieider, and H. Jakobsen, "MEMS-based uncooled infrared bolometer arrays: a review," in *MEMS/MOEMS Technologies and Applications III*, vol. 6836 of *Proceedings of SPIE*, International Society for Optics and Photonics, January 2008.

[2] M. N. Gurnee, M. Kohin, R. J. Blackwell et al., "Developments in uncooled IR technology at BAE systems," in *Infrared Technology and Applications XXVII*, vol. 4369 of *Proceedings of SPIE*, pp. 287–296, International Society for Optics and Photonics, Orlando, Fla, USA, October 2001.

[3] J. L. Tissot, C. Trouilleau, B. Fieque, A. Crastes, and O. Legras, "Uncooled microbolometer detector: recent developments at ULIS," *Opto-Electronics Review*, vol. 14, no. 1, pp. 25–32, 2006.

[4] F. Zhong, T. Dong, H. Yong, S. Yan, and K. Wang, "Void-free wafer-level adhesive bonding utilizing modified poly (diallyl phthalate)," *Journal of Micromechanics and Microengineering*, vol. 23, no. 12, Article ID 125021, 2013.

[5] E. Mottin, A. Bain, J.-L. Martin et al., "Uncooled amorphous silicon technology enhancement for 25-μm pixel pitch achievement," in *Proceedings of the International Symposium on Optical Science and Technology*, pp. 200–207, International Society for Optics and Photonics, January 2003.

[6] C. Li, C. J. Han, G. D. Skidmore, and C. Hess, "DRS uncooled VOx infrared detector development and production status," in *Infrared Technology and Applications XXXVI*, vol. 7660 of *Proceedings of SPIE*, International Society for Optics and Photonics, Orlando, Fla, USA, May 2010.

[7] B. S. Backer, N. R. Butler, M. Kohin, M. N. Gurnee, J. T. Whitwam, and T. Breen, "Recent improvements and developments in uncooled systems at BAE systems north america," in *Infrared Detectors and Focal Plane Arrays VII*, vol. 4721 of *Proceedings of SPIE*, pp. 83–90, International Society for Optics and Photonics, August 2002.

[8] S. T. Pantelides, "The electronic structure of impurities and other point defects in semiconductors," *Reviews of Modern Physics*, vol. 50, no. 4, article 797, 1978.

[9] J. Schneider, H. D. Müller, K. Maier et al., "Infrared spectra and electron spin resonance of vanadium deep level impurities in silicon carbide," *Applied Physics Letters*, vol. 56, no. 12, pp. 1184–1186, 1990.

[10] F. Niklaus, J. Pejnefors, M. Dainese et al., "Characterization of transfer-bonded silicon bolometer arrays," in *Infrared Technology and Applications XXX*, vol. 5406 of *Proceedings of SPIE*, pp. 521–530, International Society for Optics and Photonics, August 2004.

[11] L. Zhang and T. Dong, "A Si/SiGe quantum well based biosensor for direct analysis of exothermic biochemical reaction," *Journal of Micromechanics and Microengineering*, vol. 23, no. 4, Article ID 045011, 2013.

[12] B. Jiang, T. Dong, Y. Su, Y. He, and K. Wang, "Epitaxial growth and characterization of self-doping $Si_{1-x}Ge_x$/Si multi-quantum well materials," *Journal of Microelectromechanical Systems*, vol. 23, no. 1, Article ID 6558494, pp. 213–219, 2014.

[13] J. Y. Andersson, P. Ericsson, H. H. Radamson, S. G. E. Wissmar, and M. Kolahdouz, "SiGe/Si quantum structures as a thermistor material for low cost IR microbolometer focal plane arrays," *Solid-State Electronics*, vol. 60, no. 1, pp. 100–104, 2011.

[14] S. Wissmar, L. Höglund, J. Andersson, C. Vieider, S. Savage, and P. Ericsson, "High signal-to-noise ratio quantum well bolometer materials," in *Optical Materials in Defence Systems Technology III*, vol. 6401 of *Proceedings of SPIE*, International Society for Optics and Photonics, Stockholm, Sweden, September 2006.

[15] G. Hionis and G. P. Triberis, "Hole subband non-parabolicities in strained $Si/Si_{1-x}Ge_x$ quantum wells," *Superlattices and Microstructures*, vol. 24, no. 6, pp. 399–407, 1998.

[16] A. Rogalski, "Quantum well photoconductors in infrared detector technology," *Journal of Applied Physics*, vol. 93, no. 8, pp. 4355–4391, 2003.

[17] T. Zhou, T. Dong, Y. Su, and Y. He, "A cmos readout with high-precision and low-temperature-coefficient background current skimming for infrared focal plane array," *IEEE Transactions on Circuits and Systems for Video Technology*, vol. 25, no. 8, pp. 1447–1455, 2014.

[18] T. Zhou, T. Dong, Y. Su, and Y. He, "High-precision and low-cost wireless 16-channel measurement system for multi-layer thin film characterization," *Measurement*, vol. 46, no. 9, pp. 3600–3611, 2013.

Journal of
Engineering

The Scientific
World Journal
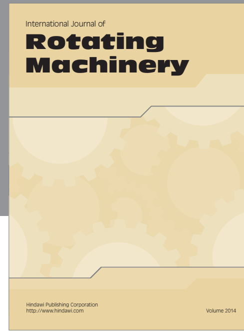
International Journal of
Rotating
Machinery
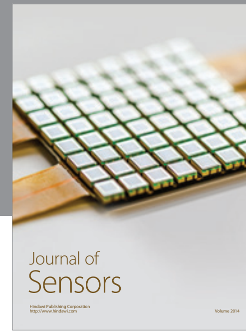
Journal of
Sensors
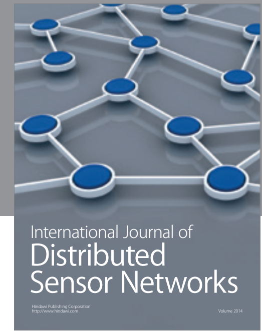
International Journal of
Distributed
Sensor Networks
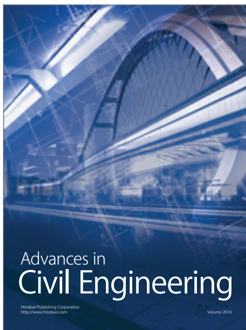
Advances in
Civil Engineering

Hindawi
Submit your manuscripts at
http://www.hindawi.com
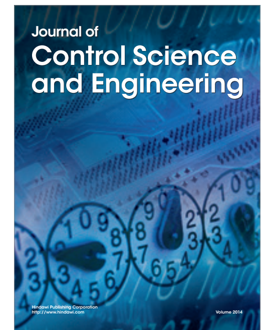
Journal of
Control Science
and Engineering

Journal of
Robotics
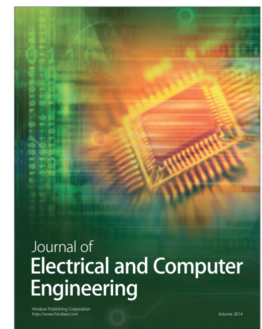
Journal of
Electrical and Computer
Engineering
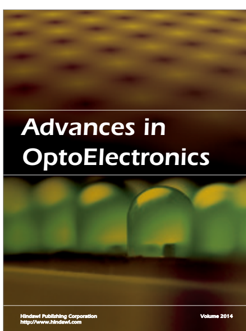
Advances in
OptoElectronics

VLSI Design

International Journal of
Navigation and
Observation
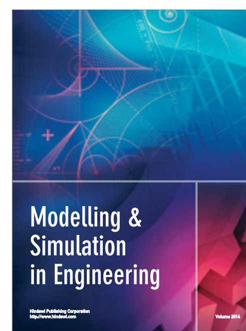
Modelling &
Simulation
in Engineering

International Journal of
Aerospace
Engineering

International Journal of
Chemical Engineering
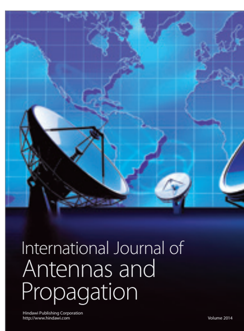
International Journal of
Antennas and
Propagation

Active and Passive
Electronic Components
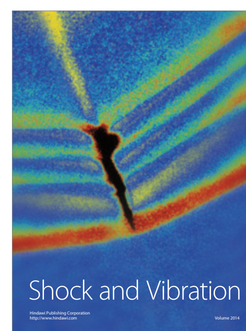
Shock and Vibration
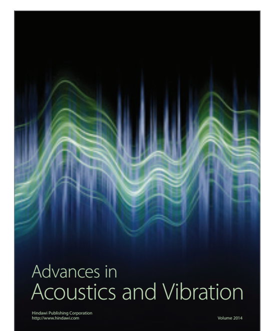
Advances in
Acoustics and Vibration